Electronic Supplementary Material (ESI) for CrystEngComm.

Electronic Supplementary Information

M. Cabello, R. Alcántara, F. Nacimiento, G. Ortiz, P. Lavela and J. L. Tirado

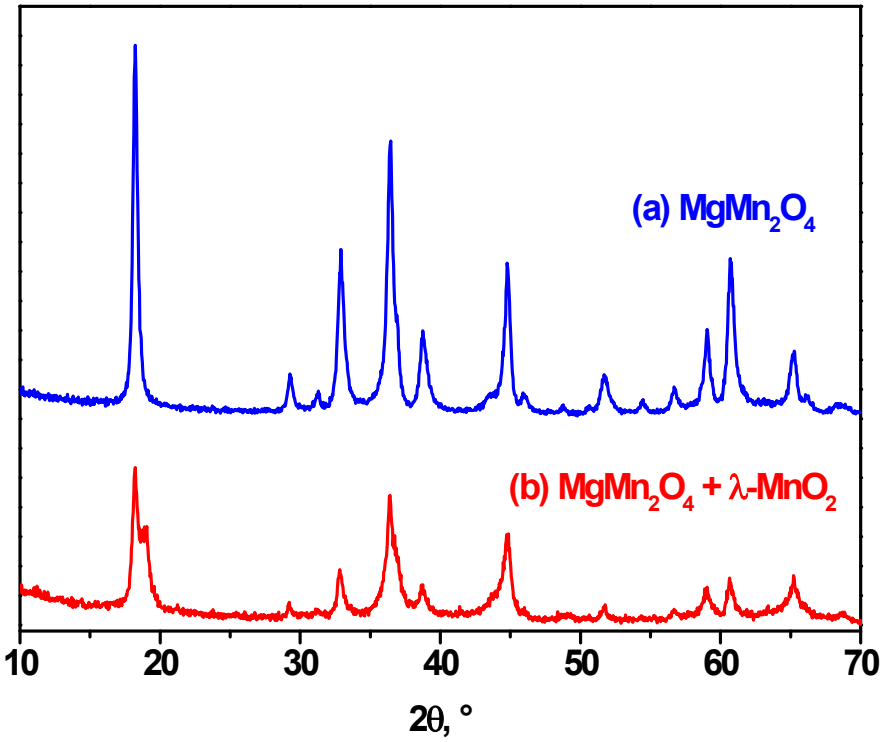

Fig S 1 X-ray diffraction patterns for tetragonal $MgMn_2O_4$ prepared at 550°C before (a) and after treatment with nitric acid at pH 2 during 50 minutes. The transformation into cubic manganese dioxide (λ-MnO_2) is only partial and the two phases coexist in (b). For the pristine sample in (a), the parameters of the tetragonal cell are: a=b=5.716(3) Å and c= 9.2867(5) Å. The cell parameters obtained from (b) are the following: for the tetragonal phase a=b=5.719(5) Å and c=9.297(2) Å, and for the cubic phase a=8.1(1) Å. This figure can be used to see comparatively how the acid treatment more easily transforms $MgMn_2O_4$ prepared at 400°C into λ-MnO_2. After acid treatment, the extraction of magnesium does not reduce the tetragonal distortion of the cell in the remaining $MgMn_2O_4$ phase. The most probably is that the texture of $MgMn_2O_4$-550°C with blocked pores hinder the acid attack and the demagnesiation is limited.

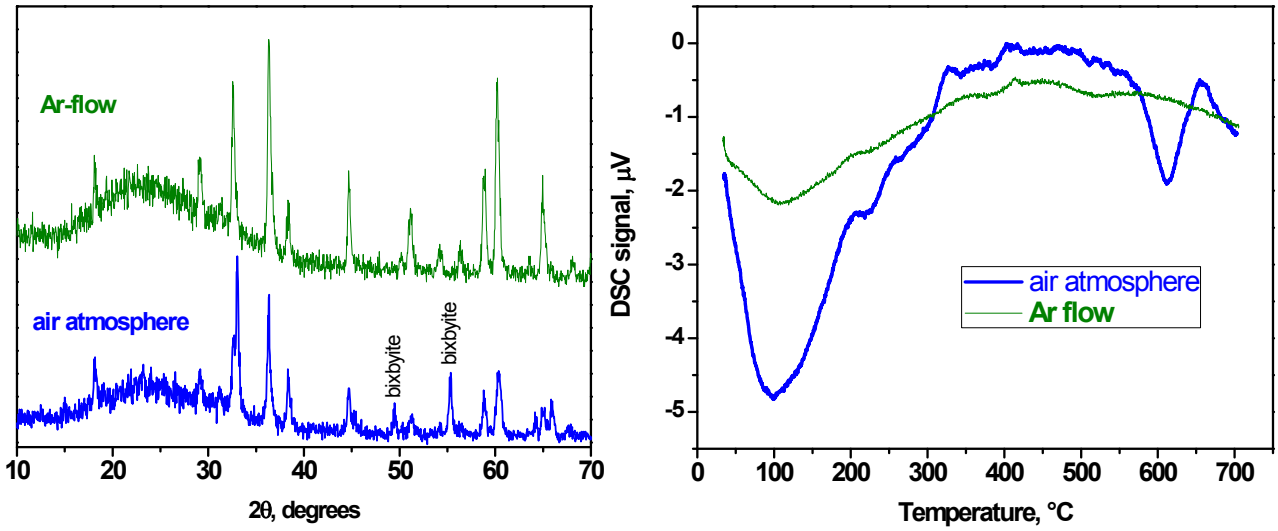

Fig S 2 XRD patterns of samples recuperated from DSC experiments (up to 700°C) that were carried out in air atmosphere and under Ar-flow starting from λ-MnO_2. Under Ar-flow the endothermal peak at 614°C is not observed and bixbyite α-Mn_2O_3 (JCPDS:41-1442) is not formed. Two Bragg reflections of the bixbyite phase are marked.

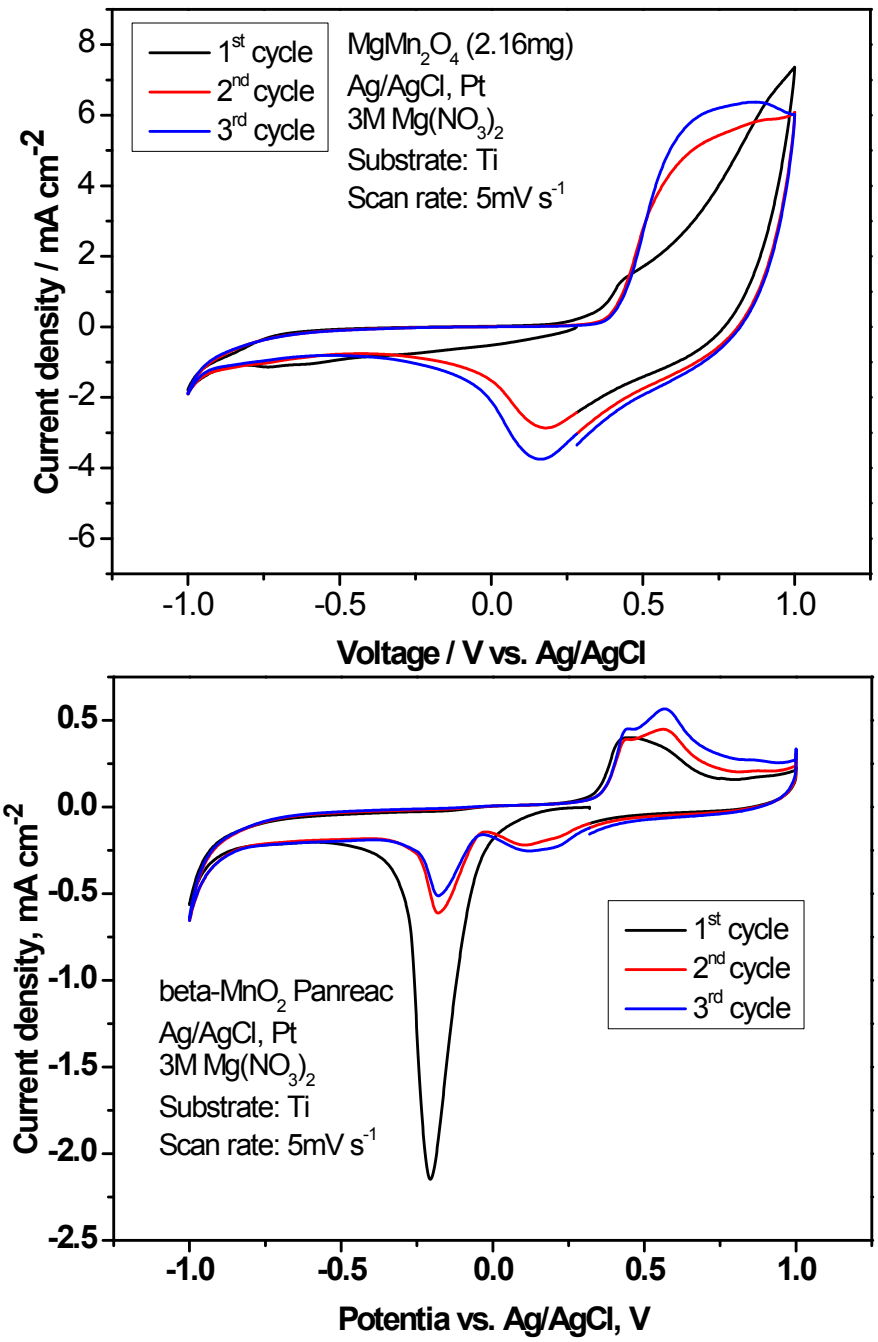

Fig S 3 Cyclic voltammetry results for 400°C-$MgMn_2O_4$ in aqueous solution. For the sake of comparison the voltammogram of pyrolusite β-MnO_2 (commercial from Panreac) si also shown. Reference electrode: Ag/AgCl. Counter electrode: Pt. Electrolyte: 3M $Mg(NO_3)_2$. Scan rate: 5mV s^{-1}. A reversible anodic/cathodic peak is observed, which is ascribed to the faradic reaction involving Mn^{3+}/Mn^{4+}. Pyrolusite phase exhibits more irreversibility and more polarization between charge and dicharge.

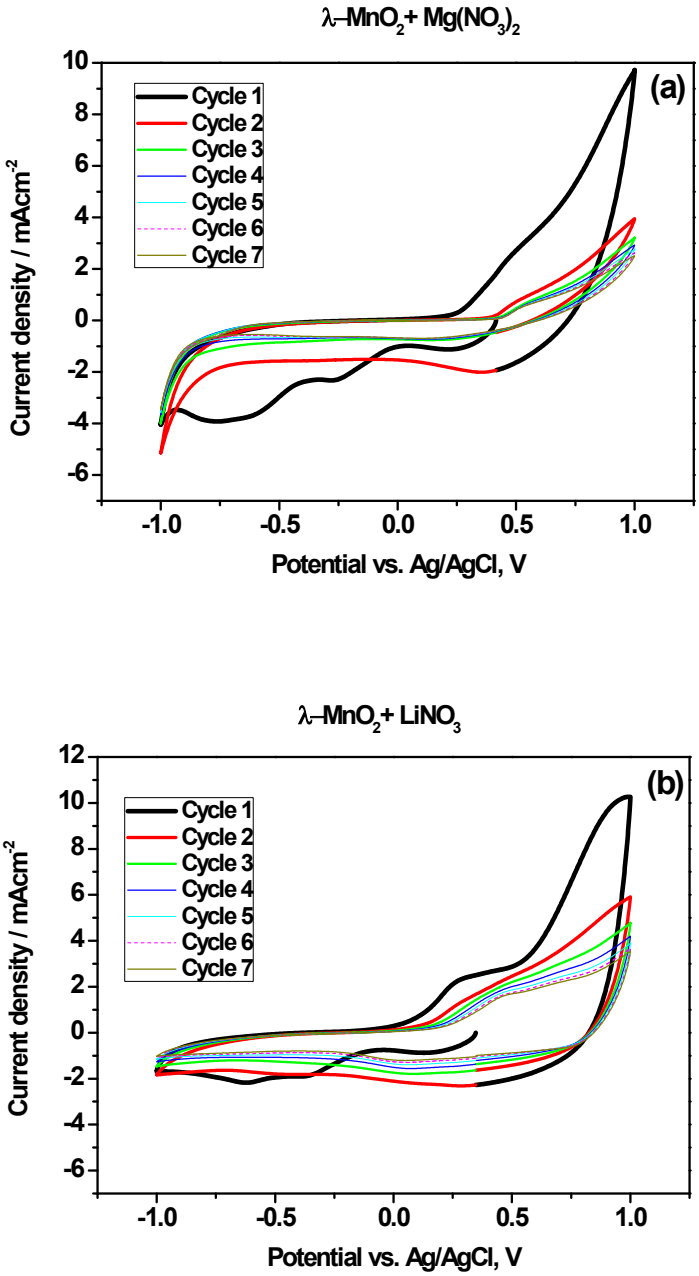

Fig S 4 Voltammetry results for λ-MnO_2 (prepared from $MgMn_2O_4$) in magnesium (a) and lithium (b) nitrate aqueous electrolyte. The corresponding XRD patterns of the cycled electrodes are shown in Fig. 8.

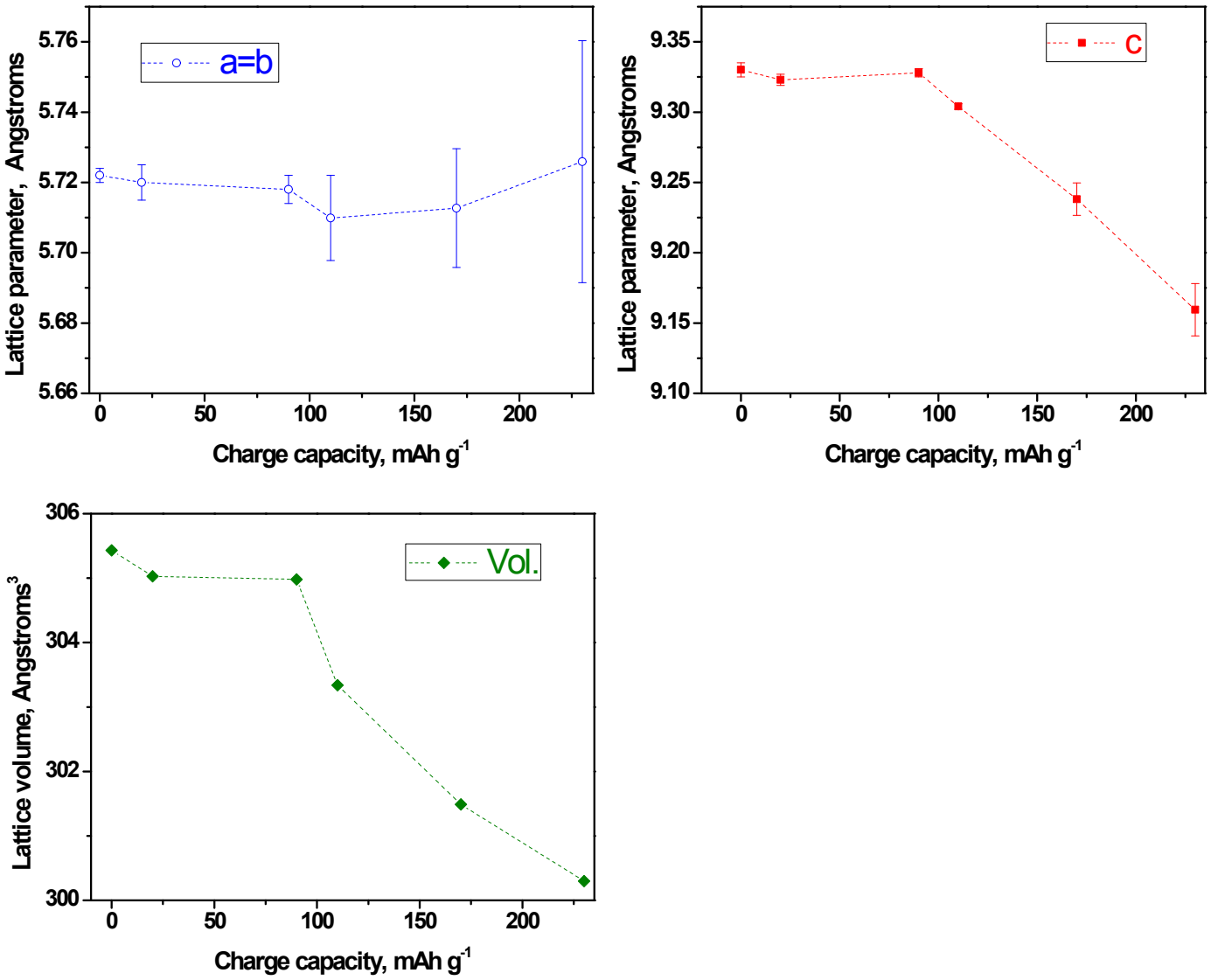

Figure S5 Lattice cell parameters (a=b and c) and lattice volume as a function of charge capacity for $MgMn_2O_4$-800°C in non-aqueous magnesium-ion battery. Electrolyte solution: 0.5 M $Mg(ClO_4)_2$ in EC:DEC (50:50). The tetragonal structure is preserved. The lattice parameters were obtaining form the ex-situ XRD of $MgMn_2O_4$ (positive) electrode recuperated from magnesium-ion batteries. The negative electrode was commercial V_2O_5. The electrodes recuperated from the electrochemical cells in the dry box and its reaction with air atmosphere during XRD recording was avoided by covering the sample with a protective plastic film.

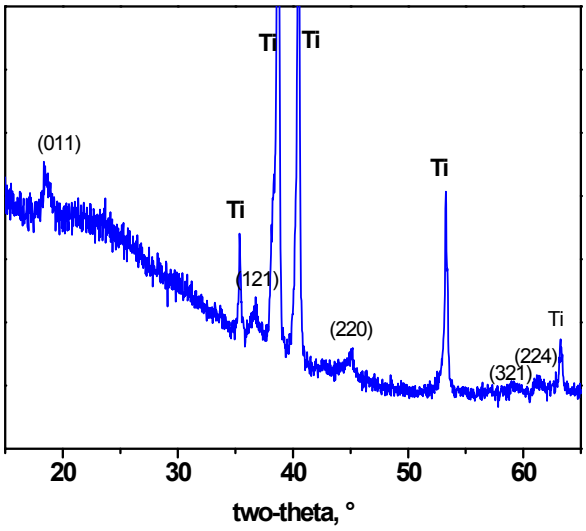

Figure S6 *Ex-situ* XRD for $MgMn_2O_4$-400°C electrode recuperated from the first charge in non-aqueous magnesium-ion battery. Electrolyte solution: 0.5 M $Mg(ClO_4)_2$ in EC:DEC (50:50). It is observed that the tetragonal structure (s.g. $I4_1/amd$) is preserved. The reflections of Ti substrate are marked.